HHS Public Access

Author manuscript

Nat Genet. Author manuscript; available in PMC 2014 August 01.

Published in final edited form as:

Nat Genet. 2014 February ; 46(2): 161–165. doi:10.1038/ng.2868.

Exome sequencing identifies BRAF mutations in papillary craniopharyngiomas

Priscilla K. Brastianos[1,2,3,4,5,22], **Amaro Taylor-Weiner**[5,22], **Peter E. Manley**[6,22], **Robert T. Jones**[4,7], **Dora Dias-Santagata**[3,8], **Aaron R. Thorner**[4,7], **Fausto J. Rodriguez**[9], **Lindsay A. Bernardo**[8], **Laura Schubert**[7], **Ashwini Sunkavalli**[7], **Nick Shillingford**[10], **Monica L. Calicchio**[10], **Hart G.W. Lidov**[3,10,11], **Hala Taha**[12], **Maria Martinez-Lage**[13], **Mariarita Santi**[14], **Phillip B. Storm**[15,16], **John Y. K. Lee**[15], **James N. Palmer**[15], **Nithin D. Adappa**[17], **R. Michael Scott**[3,18], **Ian F. Dunn**[3,19], **Edward R. Laws Jr.**[3,19], **Chip Stewart**[5], **Keith L. Ligon**[3,4,10,11], **Mai P. Hoang**[3,8], **Paul Van Hummelen**[4,7], **William C. Hahn**[3,4,5,7], **David N. Louis**[3,8], **Adam C. Resnick**[15,16], **Mark W. Kieran**[3,6,20,23], **Gad Getz**[3,5,8,23], and **Sandro Santagata**[3,10,11,21,23]

[1]Division of Hematology/Oncology, Massachusetts General Hospital, Boston, Massachusetts, USA

[2]Division of Neuro-Oncology, Massachusetts General Hospital, Boston, Massachusetts, USA

[3]Harvard Medical School, Boston, Massachusetts, USA

[4]Department of Medical Oncology, Dana-Farber Cancer Institute, Boston, Massachusetts, USA

[5]Broad Institute of MIT and Harvard, Boston, Massachusetts, USA

[6]Department of Pediatric Oncology, Dana-Farber Cancer Institute, Boston, Massachusetts, USA

Correspondence should be addressed to: P.K.B. (pbrast@broadinstitute.org), G.G. (gadgetz@broadinstitute.org) or S.S. (ssantagata@partners.org).

[22]These authors contributed equally to this work.

[23]These authors jointly directed this work.

Accession codes.

Data, including sequence data and analyses, will be available for download from the database of Genotypes and Phenotypes (dbGaP).

Note: Supplementary information is available in the online version of the paper.

Weblinks

Picard tools : http://picard.sourceforge.net
Samtools: http://samtools.sourceforge.net)
Genome Analysis Toolkit (GATK): http://www.broadinstitute.org/gatk
Firehose: http://www.broadinsitute.org/cancer/cga/firehose
Oncotator: http://www.broadinstitute.org/oncotator

AUTHOR CONTRIBUTIONS

P.K.B, P.E.M., M.W.K, G.G. and S.S. designed the study. P.K.B, A.T.W., C.S., G.G, and S.S wrote the manuscript. A.T.W., P.K.B., C.S., A.R.T. and G.G. performed computational analyses. P.V.H. supervised the sequencing. S.S. and D.N.L. reviewed the histopathology and S.S., D.N.L. and M.P.H. coordinated and reviewed the immunohistochemistry. K.L.L. managed the tissue repository. R.T.J., L.A.B., A.S, N.S and M.C. coordinated sample acquisition, processed samples and coordinated and performed exome and targeted sequencing. P.K.B., W.C.H., D.D.S., D.N.L., A.C.R., M.W.K, G.G. and S.S. supervised the study. H.G.W.L., E.R.L, I.F.D., R.M.S., P.B.S., J.Y. K. L., P.J.N., A.N.D., H.T., M.M.L., M.S., F.J.R., P.E.M., A.C.R., D.D.S., D.N.L and S.S. identified and provided materials for sequencing and validation as well as clinical information. All authors discussed the results and implications and edited the manuscript.

The author's declare no competing financial interests.

[7]Center for Cancer Genome Discovery, Dana-Farber Cancer Institute, Boston, Massachusetts, USA

[8]Department of Pathology, Massachusetts General Hospital, Boston, Massachusetts, USA

[9]Department of Pathology, Johns Hopkins University, Baltimore, Maryland, USA

[10]Department of Pathology, Boston Children's Hospital, Boston, Massachusetts, USA

[11]Department of Pathology, Brigham and Women's Hospital, Boston, Massachusetts, USA

[12]Children's Cancer Hospital Egypt 57357, Cairo, Egypt

[13]Department of Pathology and Laboratory Medicine at the Hospital of the University of Pennsylvania, Philadelphia, PA, USA

[14]Department of Pathology, Children's Hospital of Philadelphia, Philadelphia, Pennsylvania, USA

[15]Department of Neurosurgery at the Hospital of the University of Pennsylvania, Philadelphia, Pennsylvania, USA

[16]Division of Neurosurgery at the Children's Hospital of Philadelphia; Philadelphia, Pennsylvania, USA

[17]Department of Otorhinolaryngology-Head and Neck Surgery at the Hospital of the University of Pennsylvania; Philadelphia, Pennsylvania, USA

[18]Department of Neurosurgery, Boston Children's Hospital, Boston, Massachusetts, USA

[19]Department of Neurosurgery, Brigham and Women's Hospital, Boston, Massachusetts, USA

[20]Department of Pediatrics, Boston Children's Hospital, Boston, Massachusetts, USA

[21]Department of Cancer Biology, Dana-Farber Cancer Institute, Boston, Massachusetts, USA

Craniopharyngiomas are epithelial tumors that typically arise in the suprasellar region of the brain[1]. Patients experience substantial clinical sequelae both from extension of the tumors and from therapeutic interventions which damage the optic chiasm, the pituitary stalk, and the hypothalamic area[2–4]. Using whole exome sequencing we identified mutations in beta-catenin (*CTNNB1*) in nearly all adamantinomatous craniopharyngiomas (11/12; 92%) and recurrent mutations in *BRAF* (V600E) in all papillary craniopharyngiomas (3/3; 100%). Targeted genotyping revealed BRAF V600E in 95% of papillary craniopharyngiomas (36 of 39 tumors) and CTNNB1 mutation in 96% of adamantinomatous craniopharyngiomas (51 of 53 tumors). The *CTNNB1* and *BRAF* mutations were clonal in each tumor subtype and no other recurrent mutations or genomic aberrations were detected in either subtype. Adamantinomatous and papillary craniopharyngiomas harbor mutations that are mutually exclusive and clonal. These findings have important implications for the diagnosis and treatment of these neoplasms.

Craniopharyngiomas occur at an average age-adjusted incidence rate of 0.18 per 100,000[5]. There are two main subtypes of craniopharyngiomas – the adamantinomatous form that is more common in children and the papillary form that predominantly occurs in adults. Located in or above the sella turcica, craniopharyngiomas grow adjacent to the optic chiasm

and often extend to involve the hypothalamus, cranial nerves, the ventricular system, visual pathways and major blood vessels at the base of the brain. Curative surgery is exceedingly difficult[6] and resection can contribute to complications. The spectrum of complications include visual defects, severe headaches, pan-hypopituitarism, impaired intellectual function and wide-ranging hypothalamic dysfunction leading to sleep disorders[7], abnormal thermoregulation, and diabetes insipidus as well as to hyperphagia and uncontrollable obesity[2–4]. Aptly, Harvey Cushing, the father of neurosurgery, who introduced the term "craniopharyngioma" declared them "the most formidable of intracranial tumors[8,9]."

Knowledge of the molecular mechanisms that drive craniopharyngiomas remains limited, and this has hampered the development of systemic therapies for this tumor. Mutations in exon 3 of beta-catenin (*CTNNB1*), which encodes a degradation targeting motif, have been described in adamantinomatous craniopharyngiomas, occurring in 60–75% of patients in most published series[10–12]. However, mutations that drive the growth of papillary craniopharyngiomas have not been identified. To that effect, we performed massively parallel sequencing of 15 craniopharyngiomas from both subtypes and targeted genotyping in samples from 95 additional patients.

We first used whole exome sequencing to analyze the DNA from a discovery cohort of adamantinomatous (n=12) and papillary craniopharyngiomas (n=3) (Supplementary Table 1). As craniopharyngiomas are often heterogeneous tumors with nests of tumor cells interspersed between large amounts of reactive tissue and stromal cells, we expected mutations to have low allelic fractions (i.e. the mutations might only be found in a small subset of the sequenced cells due to substantial contamination by normal cells). Thus, we analyzed the sequencing data with a recently described method – MuTect – that uses a Bayesian classifier to identify somatic mutations with very low allelic fractions coupled with filters that provide high specificity[13].

In consonance with the benign histology of these tumors, we identified only a relatively small number of nonsynonymous somatic mutations in both craniopharyngioma subtypes when compared to large cohorts of other tumor types[14] (Fig. 1). The nonsynonymous mutation rate of 0.9/MB in the craniopharyngioma samples was similar to that found in a number of pediatric tumors as well as low grade tumors in adults such as WHO grade I meningioma[15] (Fig. 1). 58% of the mutations were cytosine to thymidine at CpG dinucleotides which is consistent with spontaneous deamination and not a carcinogen-induced process (Fig. 1)[14]. As anticipated, the allelic fraction for many of the mutations was very low (median 3%; range 0.96–48%).

The most frequently mutated gene was *CTNNB1*, present in 11 of 12 adamantinomatous craniopharyngiomas (Fig. 2; Supplementary Tables 2–4). These events overlapped with mutations previously described in this tumor type and were found exclusively in exon 3[10,12]. In addition, adamantinomatous craniopharyngiomas harbored isolated mutations in genes that have previously been implicated in cancer (Fig. 2). We identified mutations in genes listed in the Cancer Gene Census[16] that are involved in transcriptional regulation (*BCOR*, *CRTC3*, *MITF* and *PRDM1*) and epigenetic regulation (*KDM5A* and *SMARCA4*) as well as DNA repair (*BRCA2*) (Fig. 2). Additional mutations were detected in genes not listed in the

Cancer Gene Census but with described roles in cancer including genes involved in chromatin remodeling and regulation of transcription (including *ASCC2, KAT5, PIWIL1, SIN3A, SMC1A*), cell cycle and DNA repair (including *ATR, BARD1, CDC25B, HBP1, RBBP8, RTEL1*) and cell adhesion (*ITGA3, PKD1, PKD1L1, PODN, ROCK1, RPTN*)[16]. Many of these, however, may be 'passenger' mutations that do not contribute to tumor initiation or progression.

All three of the papillary craniopharyngiomas in our discovery set harbored mutations (c. 1799T>A) in the well-established oncogene *BRAF* (V600E) that have been shown to constitutively activate this serine-threonine kinase that regulates MAP kinase/ERK signaling and affects cell division and differentiation (Fig. 2). None of the three papillary craniopharyngiomas had mutations in *CTNNB1*. Although two of these samples were resected from adults (31 and 52 years old), one of the samples was from a rare papillary craniopharyngioma that occurred in a child (9 years old) suggesting a similar pathogenesis between pediatric and adult papillary craniopharyngiomas. In these tumors, we did not identify mutations in other genes listed in the Cancer Gene Census but did note isolated mutations in other genes with potential roles in cancer including ones encoding chromatin remodeling factors (*CHD5, CHD6*)[17] and cell adhesion molecules (*CDH26, PTPRT*)[18], and one (KIAA1549) that is fused to *BRAF* in most cases of pilocytic astrocytoma[19,20]. These mutations, like some of those found in adamantinomatous craniopharyngiomas, may also be 'passenger' mutations.

MutSig[14] was used to analyze the list of mutations identified in our discovery cohort of 15 cases to identify genes that are significantly mutated. Although our cohort is small compared to those from other genomic studies[14] (Fig. 1), the prevalence of mutations in *CTNNB1* and *BRAF* was so high that these mutations were readily detected as statistically significant (Fig. 2).

To validate our findings, we used targeted genotyping approaches to analyze an additional 98 craniopharyngioma samples (from 95 different patients) for mutations in the most commonly mutated genes in our discovery cohort – *BRAF* and *CTNNB1*. We also performed immunohistochemistry (IHC) using an antibody (VE1) that selectively recognizes the BRAF V600E mutant epitope and not the wild-type epitope from BRAF[21]. In addition, we evaluated the activation status of beta-catenin using an antibody that allowed us to detect nuclear (activated) and membranous (inactivated) beta-catenin[12]. In total, our validation cohort consisted of 39 papillary craniopharyngioma tumors from 36 different patients and 59 adamantinomatous craniopharyngioma tumors, each from different patients (Supplementary Table 1). While *CTNNB1* mutations were detected in the adamantinomatous craniopharyngioma samples (51 of 53 samples, 96%), none of these samples harbored *BRAF* mutations (neither V600E, D, L, M nor K). Cytoplasmic and nuclear beta-catenin was identified by IHC in all of the adamantinomatous samples tested but beta-catenin was exclusively localized to the cytoplasmic membrane in all papillary craniopharyngioma samples tested (Supplementary Table 1, Fig. 3). Remarkably, by targeted genotyping and IHC we detected V600E mutations in 34 of the 36 patients with papillary craniopharyngiomas (94.4%) (Supplementary Table 1).

The allelic fraction of mutations (including those in *BRAF* and *CTNNB1*) in our whole exome data was low (Fig. 2a, **middle panel**, Supplementary Table 2). This raised the possibility of genetic heterogeneity in our tumor samples. To assess this, we used a recently developed computational method (see Methods section) that corrects for tumor purity and estimates the fraction of cancer cell nuclei that harbor a particular mutation (cancer cell fraction; CCF). Although these methods demonstrated that most of the somatic mutations identified in our samples were indeed subclonal, we found that the *BRAF* and *CTNNB1* mutations were clonal (i.e. present in all tumor cells) in the analyzed samples (Fig. 2a **upper panel**, Fig. 4a **and** Supplementary Table 2-column BB).

To further validate our analysis of intra-tumor heterogeneity, we reviewed the pattern and distribution of BRAF staining in the craniopharyngioma samples (Supplementary Table 1). Using the BRAF V600E selective antibody, we did not detect BRAF V600E in the adamantinomatous craniopharyngioma samples (Supplementary Table 1) nor in two of the papillary craniopharyngioma samples with wild type *BRAF* that we tested (Fig. 4b). In the genetically confirmed BRAF V600E mutant samples, however, we observed widespread immunoreactivity across the tumor cell population. In these samples, lymphocytes and stromal cells of the fibrovascular core of the tumors were not immunoreactive, but the squamopapillary tumor epithelium stained diffusely for BRAF V600E. This observation supports the conclusion that *BRAF* mutations are present uniformly throughout the neoplastic epithelial cells.

Our whole exome sequencing data of craniopharyngiomas demonstrates that the adamantinomatous and papillary subtypes have distinct molecular underpinnings, each principally driven by mutations in a single well-established oncogene – *CTNNB1* (beta-catenin) in the adamantinomatous form and *BRAF* in the papillary form, independent of age.

These mutations appear to be critical events in the pathogenesis of these tumors for several reasons. First, the high prevalence of mutations in *CTNNB1* and *BRAF* in craniopharyngiomas occurs amongst an overall paucity of additional mutations, supporting that these are likely instrumental to the growth of these tumors. Second, the mutations are clonal and perfectly segregate with their respective histologic subtypes indicating that these are defining genetic aberrations. Moreover, the frequency of *CTNNB1* mutations and *BRAF* mutations are much higher in craniopharyngiomas than in most other tumor types that bear these mutations.

Given the mutual exclusivity of *BRAF* and *CTNNB1* mutations, immunohistochemistry for BRAF V600E and beta-catenin could be used to routinely distinguish papillary from adamantinomatous craniopharyngiomas, and thereby direct patients to appropriate clinical trials. While agents that target WNT signaling remain in development[22,23], the availability of BRAF inhibitors such as vemurafenib[24–29] and dabrafenib[30,31] suggests that patients with papillary craniopharyngiomas could immediately benefit from such targeted therapeutics. These agents have shown a robust clinical response against BRAF V600E mutant melanomas[25] and hairy cell leukemias[32] as well as brain tumors such as pleomorphic xanthoastrocytoma[33,34] and ganglioglioma[34,35]. Trials of these therapeutics for papillary craniopharyngiomas should be explored in patients with either residual or recurrent tumor

following surgical resection. Also, BRAF inhibitors could be evaluated as first-line therapy, prior to surgical resection or radiation therapy.

In summary, our discovery of frequent and clonal mutations in adamantinomatous and papillary craniopharyngioma in *CTNNB1* and *BRAF*, respectively, offers valuable opportunities for testing molecularly guided therapeutics for the treatment of these formidable brain tumors.

ONLINE METHODS

Sample Selection and Preparation

The study was reviewed and approved by the human subjects institutional review boards of the Dana-Farber Cancer Institute, Brigham and Women's Hospital, Broad Institute of Harvard and MIT, Boston Children's Hospital, Johns Hopkins Hospital, Children's Cancer Hospital Egypt, and Children's Hospital of Philadelphia. Written informed consent was obtained from all participants whose tumor samples were subjected to whole-exome sequencing. Histologic diagnosis was re-confirmed on all samples by a board certified neuropathologist (S.S.) and representative fresh-frozen and paraffin embedded blocks with estimated purity of ≥10% were selected. DNA was extracted from tissue shavings of frozen tissue or 1 mm core punch biopsies (Miltex, cat# 33-31AA-P/25) from FFPE tissue and from buffy coat preparations of paired blood using standard techniques (QIAGEN, Valencia CA). The DNA was then quantified using PicoGreen® dye (InVitrogen, Carlsbad CA). Mass spectrometric genotyping with a well-established 48-SNP panel was used to confirm the identity of tumor-normal pairs (Sequenom, San Diego CA)[36].

Whole Exome Sequencing and Analyses

Whole exome sequencing was performed as previously described[15]. In brief, DNA was fragmented by sonication (Covaris Inc., Woburn, MA) to 150 bp and further purified using Agencourt AMPure XP beads. 50 ng size selected DNA was then ligated to specific adaptors during library preparation (Illumina TruSeq, Illumina Inc, San Diego, CA). Each library was made with sample specific barcodes, quantified by QPCR (Kapa Biosystems, Inc, Woburn, MA) and 2 libraries were pooled to a total of 500 ng for exome enrichment using the Agilent SureSelect hybrid capture kit (Whole Exome_v2 and Whole Exome_v4, 44 Mb; Agilent Technologies, Santa Clara, CA). Several captures were pooled further and sequenced in one or more lanes to a final equivalent of 2 exomes per lane on a Hiseq 2500 (Illumina Inc, San Diego, CA).

Read pairs were aligned to the hg19 reference sequence using the Burrows-Wheeler Aligner[37] and sample reads were de-multiplexed using Picard tools. Data were sorted and duplicate-marked using Samtools and Picard. Bias in base quality score assignments due to flowcell, lane, dinucleotide context, and machine cycle were analyzed and recalibrated, and local realignment around insertions/deletions was achieved using the Genome Analysis Toolkit (GATK)[38,39]. Somatic variant calling was performed within the Firehose environment[40] using MuTect[13]. All sample pairs passed a QC pipeline to test for any tumor/

normal and inter-individual mix-ups by comparing insert-size distribution and copy-number profile as described previously[41].

Somatic mutations and short insertions/deletions were called and post-filtered using MuTect[13] and IndelLocator[40,41]. These were annotated to genes and compared to events in the Catalogue of Somatic Mutations in Cancer (COSMIC) using Oncotator, and spurious calls caused by mis-mapping and other previously identified systematic errors were removed using an established list of known problematic sites[15,40,42,43]. MutSig[14] was used to determine the significance of mutated genes. MutSig compares observed mutations against expected sequence specific, context-specific, tumor-specific and gene specific background mutation frequencies. Additionally MutSig prioritizes mutations that are positionally clustered or occur in highly conserved regions[40,42,43]. We analyzed mutational spectra and rate across multiple tumor types using previously described methods[14].

Mutation clonality analysis

To assess whether mutations are clonal (i.e. present in all cancer cells), we assessed the cancer cell fraction (CCF) of each mutation, as described in Carter et al[44]. Mutations for which the CCF is close to 1 are considered clonal. Those mutations with lower probable CCFs are considered subclonal. To determine the CCF we first calculated the sample purity (i.e. the percentage of tumor cells in our sample) by constructing the probability density function for the allele fractions of mutations. Using that information we then identified a clonal heterozygous peak at or below 0.5 allele fraction:

$$pdf(af) = \sum_{m} betapdf(af, alt(m)+1, ref(m)+1)$$

where af is the true allele fraction between 0 and 1, alt is the alternate allele counts, ref is the reference allele counts, m is the index for mutation count[44]. We assumed local copy number at each mutation is two for craniopharyngioma and that each tumor has heterozygous clonal mutations that are sufficient to form a peak[45,46]. Given these assumptions purity is peak af * 2.

Once we had estimated tumor purity we then estimated the cancer cell fraction (CCF) for each mutation. The cancer cell fraction is the percentage of tumor cells harboring a given mutation. Clonal mutations have a true cancer cell fraction of one and subclonal mutations have a true cancer cell fraction of less than one. The observed allele counts correspond to a probability density of the CCF and this can be estimated with the following equation:[44]

$$pdf(CCF, m) = betapdf\left(\frac{CCF}{CN(m)} * purity, alt(m)+1, ref(m)+1\right)$$

where CN(m) is the local copy number at the given mutation m, and CCF ranges from 0 to 1. The probability for any allele fraction greater than the maximum CCF allowed was folded back to a CCF of 1. We assumed again a copy number of two[26,27]. We also considered the possibility that the site is homozygous in both copies of the chromosome (loss of

heterozygosity) by multiplying the CCF by 2 in the equation above and chose the solution with the highest peak probability. The CCF formulation is approximately equivalent to ABSOLUTE[44]. The pdfs also provided a direct estimate of the confidence intervals on CCF. Each mutation was classified as clonal or subclonal based on the probability that the CCF exceeded 0.80. A probability threshold of 0.5 was used throughout for this classification[47].

Validation of Candidate Mutations by Sequenom Genotyping and Snapshot

We validated all of the common mutations in *BRAF* and *CTNNB1* by mass spectrometric genotyping based on the Sequenom MassARRAY® technology (Sequenom Inc, San Diego, CA) using a multi-base homogenous Mass-Extend (hME) as previously described[35,48]. The complete hME assay list is provided in the supplementary appendix. A second targeted sequencing platform (SNaPshot genotyping) was performed as previously described to validate the BRAF V600E (c.1799T>A) mutation in all papillary craniopharyngiomas[33,49,50].

Immunohistochemistry

We performed immunohistochemical studies on five-micrometer-thick whole tissue sections of formalin-fixed, paraffin-embedded tissue in a Bond 3 automated immunostainer (Leica Microsystems, Bannockburn, IL, USA) using a primary antibody against BRAF V600E (clone: VE1, 1:100, Spring Bioscience, Pleasanton, CA) and a primary antibody against beta-catenin. For BRAF V600E, we deparaffinized the sections on the Leica Bond using Bond Dewax solution and performed antigen retrieval with an EDTA-based solution (Leica) at pH 9 and Leica Polymer Refine Kit for DAB (Diaminobenzidine) staining. Appropriate positive and negative controls were included. Positive staining was characterized by diffuse and moderate cytoplasmic staining of the tumor cells. We considered isolated nuclear staining, weak staining of occasional cells, or faint diffuse staining as negative staining. For beta-catenin (BD pharmigen, cat# 610154, mouse-monoclonal, clone: 14), antigen retrieval was performed in a pressure cooker in citrate buffer (pH=6.0, 1:1000 dilution) with a 45 minute incubation followed by Dako anti-mouse-HRP for 30 minutes at room temperature. Cases with nuclear staining (which ranged from low level to high level) were scored as positive and membranous staining were scored as negative.

Supplementary Material

Refer to Web version on PubMed Central for supplementary material.

ACKNOWLEDGEMENTS

The authors would like to thank Matthew Ducar for his assistance with genomic analyses; Sara Chauvin for project management; Loreal Brown and Hayley Malkin for assisting with sample collection; Terri Woo, Ben Rich, Revaz Machaidze and Dan Feldman for technical assistance; Michael Lawrence for design of Figure 1; Nico Stransky for design of Figure 2A; and Hermes Taylor-Weiner and Charilaos H. Brastianos for critical review of the manuscript. This work was supported by the Jared Branfman Sunflowers for Life Fund for Pediatric Brain and Spinal Cancer Research, and the Pediatric Low-Grade Astrocytoma (PLGA) Program (S.S., W.C.H., and to Charles D. Stiles), Pedals for Pediatrics and the Clark Family (P.E.M., M.W.K.), the Stahl Family Charitable Foundation (P.E.M), the Stop&Shop Pediatric Brain Tumor Program (P.E.M., M.W.K.), the Pediatric Brain Tumor Clinical and Research Fund (P.E.M., M.W.K.), as well as by the V Foundation (S.S.). S.S. is supported by K08 NS064168 and P.K.B by K12 CA090354-11, the Brain Science Foundation, Susan G. Komen for the Cure, Terri Brodeur Breast Cancer Foundation, Conquer Cancer Foundation and the American Brain Tumor Association.

REFERENCES

1. Louis, DN.; Ohgaki, H.; Wiestler, OD.; Cavenee, WK. International Agency for Research on Cancer; 2007. WHO Classification of Tumours of the Central Nervous System; p. 238-240.
2. Crotty TB, et al. Papillary craniopharyngioma: a clinicopathological study of 48 cases. J Neurosurg. 1995; 83:206–214. [PubMed: 7616262]
3. Duff J, et al. Long-term outcomes for surgically resected craniopharyngiomas. Neurosurgery. 2000; 46:291–302. discussion 302–5. [PubMed: 10690718]
4. Weiner HL, et al. Craniopharyngiomas: a clinicopathological analysis of factors predictive of recurrence and functional outcome. Neurosurgery. 1994; 35:1001–1010. discussion 1010–1. [PubMed: 7885544]
5. Dolecek TA, Propp JM, Stroup NE, Kruchko C. CBTRUS statistical report: primary brain and central nervous system tumors diagnosed in the United States in 2005–2009. Neuro Oncol. 2012; 14(Suppl 5):v1–v49. [PubMed: 23095881]
6. Liubinas SV, Munshey AS, Kaye AH. Management of recurrent craniopharyngioma. J Clin Neurosci. 2011; 18:451–457. [PubMed: 21316970]
7. Manley PE, et al. Sleep dysfunction in long term survivors of craniopharyngioma. J Neurooncol. 2012; 108:543–549. [PubMed: 22528788]
8. Barkhoudarian G, Laws ER. Craniopharyngioma: history. Pituitary. 2013; 16:1–8. [PubMed: 22744873]
9. Cushing H. Intracranial tumors: notes upon a series of two thousand cases with surgical mortality percentages pertaining thereto. 1932
10. Buslei R, et al. Common mutations of beta-catenin in adamantinomatous craniopharyngiomas but not in other tumours originating from the sellar region. Acta Neuropathol. 2005; 109:589–597. [PubMed: 15891929]
11. Kato K, et al. Possible linkage between specific histological structures and aberrant reactivation of the Wnt pathway in adamantinomatous craniopharyngioma. J Pathol. 2004; 203:814–821. [PubMed: 15221941]
12. Sekine S, et al. Craniopharyngiomas of adamantinomatous type harbor beta-catenin gene mutations. Am J Pathol. 2002; 161:1997–2001. [PubMed: 12466115]
13. Cibulskis K, et al. Sensitive detection of somatic point mutations in impure and heterogeneous cancer samples. Nat Biotechnol. 2013; 31:213–219. [PubMed: 23396013]
14. Lawrence MS, et al. Mutational heterogeneity in cancer and the search for new cancer-associated genes. Nature. 2013; 499:214–218. [PubMed: 23770567]
15. Brastianos PK, et al. Genomic sequencing of meningiomas identifies oncogenic SMO and AKT1 mutations. Nat Genet. 2013; 45:285–289. [PubMed: 23334667]
16. Futreal PA, et al. A census of human cancer genes. Nat Rev Cancer. 2004; 4:177–183. [PubMed: 14993899]
17. Stanley FK, Moore S, Goodarzi AA. CHD chromatin remodelling enzymes and the DNA damage response. Mutat Res. 2013
18. Laczmanska I, Sasiadek MM. Tyrosine phosphatases as a superfamily of tumor suppressors in colorectal cancer. Acta Biochim Pol. 2011; 58:467–470. [PubMed: 22146137]
19. Jones DT, et al. Oncogenic RAF1 rearrangement and a novel BRAF mutation as alternatives to KIAA1549:BRAF fusion in activating the MAPK pathway in pilocytic astrocytoma. Oncogene. 2009; 28:2119–2123. [PubMed: 19363522]
20. Tian Y, et al. Detection of KIAA1549-BRAF fusion transcripts in formalin-fixed paraffin-embedded pediatric low-grade gliomas. J Mol Diagn. 2011; 13:669–677. [PubMed: 21884820]
21. Capper D, et al. Assessment of BRAF V600E mutation status by immunohistochemistry with a mutation-specific monoclonal antibody. Acta Neuropathol. 2011; 122:11–19. [PubMed: 21638088]
22. Anastas JN, Moon RT. WNT signalling pathways as therapeutic targets in cancer. Nat Rev Cancer. 2013; 13:11–26. [PubMed: 23258168]

23. Basu A, et al. An interactive resource to identify cancer genetic and lineage dependencies targeted by small molecules. Cell. 2013; 154:1151–1161. [PubMed: 23993102]
24. Chapman PB, et al. Improved survival with vemurafenib in melanoma with BRAF V600E mutation. N Engl J Med. 2011; 364:2507–2516. [PubMed: 21639808]
25. Flaherty KT, et al. Inhibition of mutated, activated BRAF in metastatic melanoma. N Engl J Med. 2010; 363:809–819. [PubMed: 20818844]
26. Ribas A, Flaherty KT. BRAF targeted therapy changes the treatment paradigm in melanoma. Nat Rev Clin Oncol. 2011; 8:426–433. [PubMed: 21606968]
27. Sosman JA, et al. Survival in BRAF V600-mutant advanced melanoma treated with vemurafenib. N Engl J Med. 2012; 366:707–714. [PubMed: 22356324]
28. Chamberlain MC. Salvage therapy with BRAF inhibitors for recurrent pleomorphic xanthoastrocytoma: a retrospective case series. J Neurooncol. 2013; 114:237–240. [PubMed: 23756728]
29. Rush S, Foreman N, Liu A. Brainstem ganglioglioma successfully treated with vemurafenib. J Clin Oncol. 2013; 31:e159–e160. [PubMed: 23358987]
30. Ascierto PA, et al. Phase II Trial (BREAK-2) of the BRAF Inhibitor Dabrafenib (GSK2118436) in Patients With Metastatic Melanoma. J Clin Oncol. 2013
31. Sievert AJ, et al. Paradoxical activation and RAF inhibitor resistance of BRAF protein kinase fusions characterizing pediatric astrocytomas. Proc Natl Acad Sci U S A. 2013; 110:5957–5962. [PubMed: 23533272]
32. Dietrich S, et al. BRAF inhibition in refractory hairy-cell leukemia. N Engl J Med. 2012; 366:2038–2040. [PubMed: 22621641]
33. Dias-Santagata D, et al. BRAF V600E mutations are common in pleomorphic xanthoastrocytoma: diagnostic and therapeutic implications. PLoS One. 2011; 6:e17948. [PubMed: 21479234]
34. Schindler G, et al. Analysis of BRAF V600E mutation in 1,320 nervous system tumors reveals high mutation frequencies in pleomorphic xanthoastrocytoma, ganglioglioma and extra-cerebellar pilocytic astrocytoma. Acta Neuropathol. 2011; 121:397–405. [PubMed: 21274720]
35. MacConaill LE, et al. Profiling critical cancer gene mutations in clinical tumor samples. PLoS One. 2009; 4:e7887. [PubMed: 19924296]
36. Demichelis F, et al. SNP panel identification assay (SPIA): a genetic-based assay for the identification of cell lines. Nucleic Acids Res. 2008; 36:2446–2456. [PubMed: 18304946]
37. Li H, Durbin R. Fast and accurate short read alignment with Burrows-Wheeler transform. Bioinformatics. 2009; 25:1754–1760. [PubMed: 19451168]
38. DePristo MA, et al. A framework for variation discovery and genotyping using next-generation DNA sequencing data. Nature genetics. 2011; 43:491–498. [PubMed: 21478889]
39. McKenna A, et al. The Genome Analysis Toolkit: a MapReduce framework for analyzing next-generation DNA sequencing data. Genome research. 2010; 20:1297–1303. [PubMed: 20644199]
40. Chapman MA, et al. Initial genome sequencing and analysis of multiple myeloma. Nature. 2011; 471:467–472. [PubMed: 21430775]
41. Berger MF, et al. The genomic complexity of primary human prostate cancer. Nature. 2011; 470:214–220. [PubMed: 21307934]
42. Lohr JG, et al. Discovery and prioritization of somatic mutations in diffuse large B-cell lymphoma (DLBCL) by whole-exome sequencing. Proceedings of the National Academy of Sciences of the United States of America. 2012; 109:3879–3884. [PubMed: 22343534]
43. Stransky N, et al. The mutational landscape of head and neck squamous cell carcinoma. Science. 2011; 333:1157–1160. [PubMed: 21798893]
44. Carter SL, et al. Absolute quantification of somatic DNA alterations in human cancer. Nat Biotechnol. 2012; 30:413–421. [PubMed: 22544022]
45. Rickert CH, Paulus W. Lack of chromosomal imbalances in adamantinomatous and papillary craniopharyngiomas. J Neurol Neurosurg Psychiatry. 2003; 74:260–261. [PubMed: 12531965]
46. Yoshimoto M, et al. Comparative genomic hybridization analysis of pediatric adamantinomatous craniopharyngiomas and a review of the literature. J Neurosurg. 2004; 101:85–90. [PubMed: 16206977]

47. Landau DA, et al. Evolution and impact of subclonal mutations in chronic lymphocytic leukemia. Cell. 2013; 152:714–726. [PubMed: 23415222]

48. Thomas RK, et al. High-throughput oncogene mutation profiling in human cancer. Nat Genet. 2007; 39:347–351. [PubMed: 17293865]

49. Corcoran RB, et al. BRAF gene amplification can promote acquired resistance to MEK inhibitors in cancer cells harboring the BRAF V600E mutation. Sci Signal. 2010; 3:ra84. [PubMed: 21098728]

50. Dias-Santagata D, et al. Rapid targeted mutational analysis of human tumours: a clinical platform to guide personalized cancer medicine. EMBO Mol Med. 2010; 2:146–158. [PubMed: 20432502]

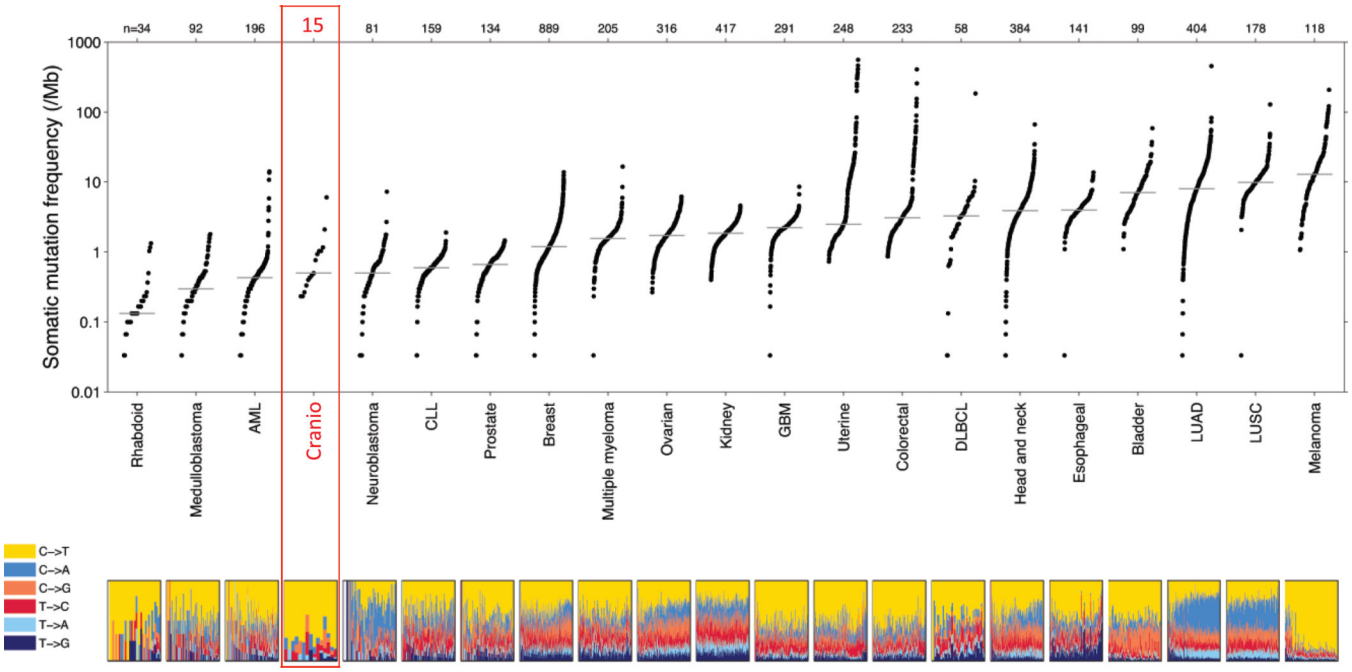

Figure 1.

Plot of the number of non-synonymous mutations per megabase in craniopharyngiomas in comparison to a broad range of pediatric and adult tumors. Data for all other tumor types, as well as the figure design were taken from Lawrence et al[14]. Each dot in this plot corresponds to a matched tumor–normal pair. The vertical position indicates the frequency of somatic mutations in that exome. Tumor types are ordered based on their median non-synonymous frequency and within each tumor type tumor-normal pairs are ordered from lowest to highest frequency. The relative proportions of six different possible base-pair substitutions are indicated in the bottom panel. Craniopharyngioma data are derived from whole exome sequencing of 15 tumor-normal pairs including 12 adamantinomatous and 3 papillary craniopharyngioma and marked in red. AML – Acute myelogenous leukemia, Cranio – Craniopharyngioma, DLBCL – Diffuse large B-cell lymphoma, LUAD – Lung adenocarcinoma; LUSC – Lung squamous cell carcinoma.

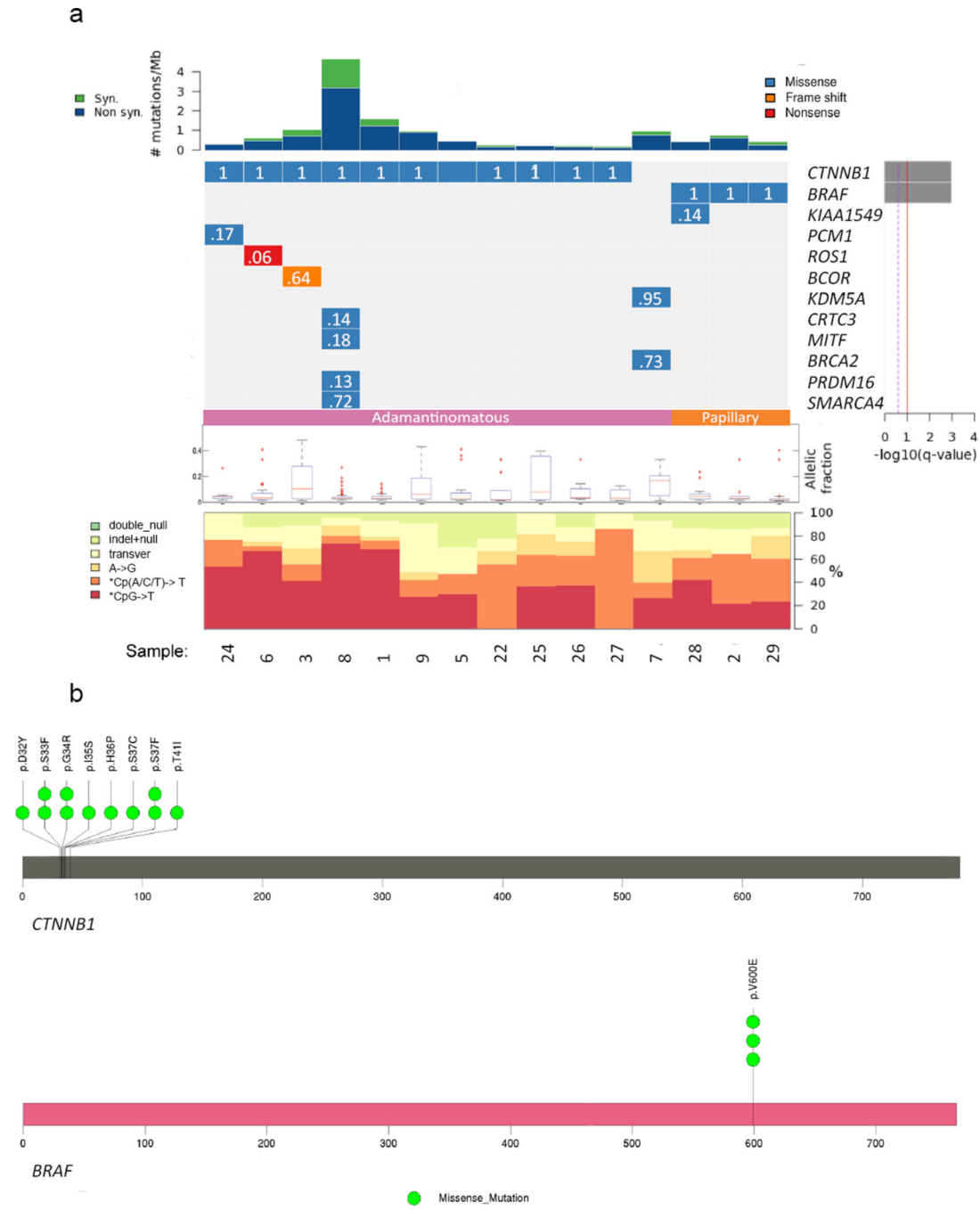

Figure 2.

Mutations in adamantinomatous and papillary craniopharyngiomas. Panel a depicts the number of mutations per megabase in each of 15 craniopharyngioma whole exome sequencing data sets (12 adamantinomatous and 3 papillary samples). Specific genes are listed bearing non-synonymous somatic mutations in genes listed in Cancer Gene Census[16]. At the right we show the false discovery rate q-values providing the significance of mutations in each listed gene. Cancer relevant genes that are not listed in the Cancer Gene Census are not shown. The q value is an evaluation of whether a gene is significantly

mutated above the expected basal rate of mutation. The q values for BRAF and CTNNB1 are <0.00001. The q values of other genes in the plot are equal to 1. A full list of mutated genes is provided in Supplementary Table 2. Colors indicate the type of genetic change identified. Only one mutation is indicated even if multiple mutations were found in a particular gene. The cancer cell fraction (CCF, 0–1.0) for each indicated mutation is shown in white type in the corresponding box. The allelic fraction for mutations in each sample is shown in box plots with the median indicated by a red line (the allelic fraction for each mutation is listed in Supplementary Table 2. For each sample, the relative frequencies of six different possible base-pair substitutions are presented in the bottom panel. In Panel b, schematics for *CTNNB1* and *BRAF* indicating the location of identified mutations (11 in *CTNNB1* and 3 in *BRAF*) are shown.

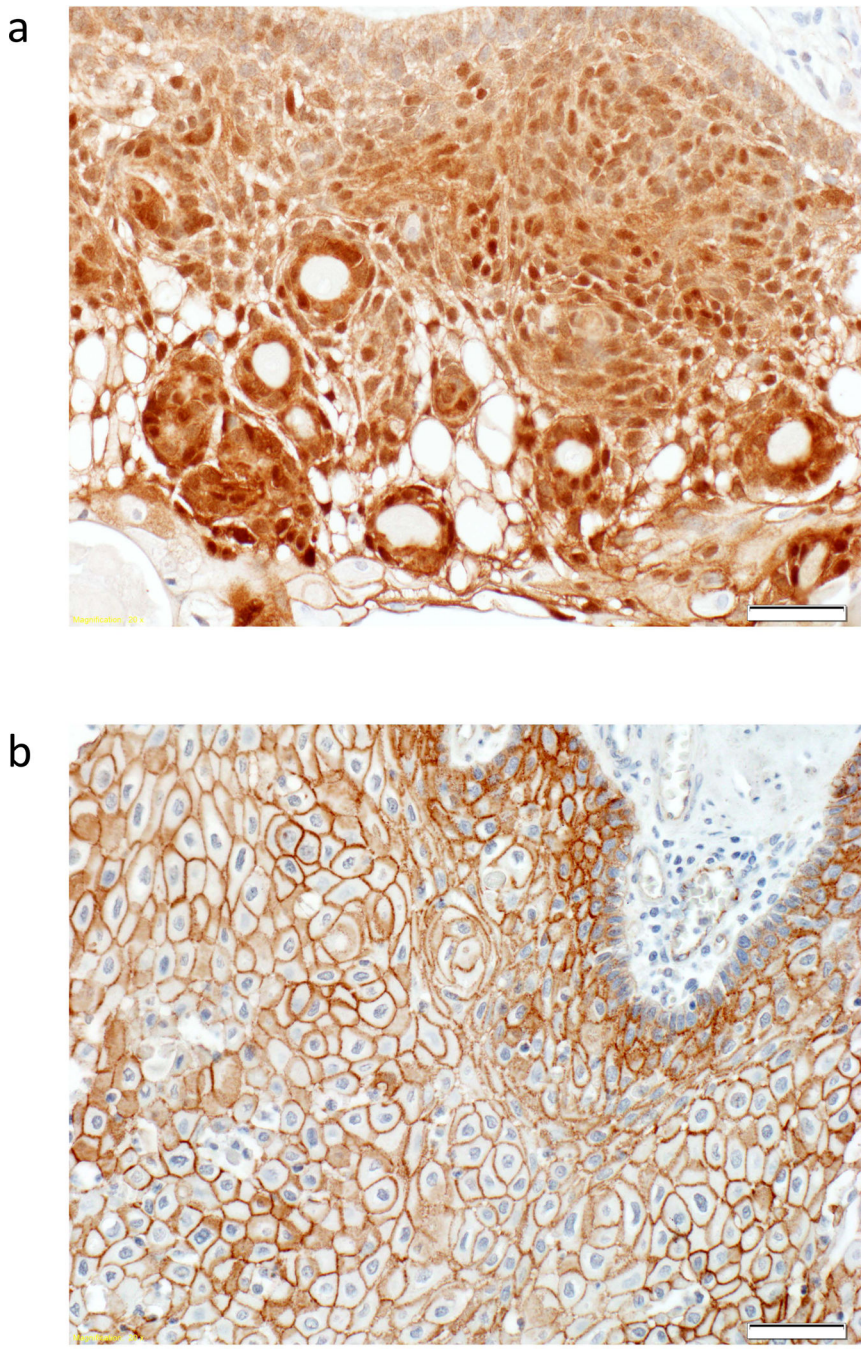

Figure 3.

Beta-catenin localization is different in adamantinomatous and papillary craniopharyngiomas. Immunohistochemistry for beta-catenin was performed. In Panel a, beta-catenin is localized to the cytoplasm and the nucleus in an adamantinomatous craniopharyngioma. In Panel b, beta catenin is localized to the cell membrane in a papillary craniopharyngioma. Scale bars, 50 μm. Beta-catenin localization in many samples from the discovery and validation cohort is reported in Supplementary Table 1.

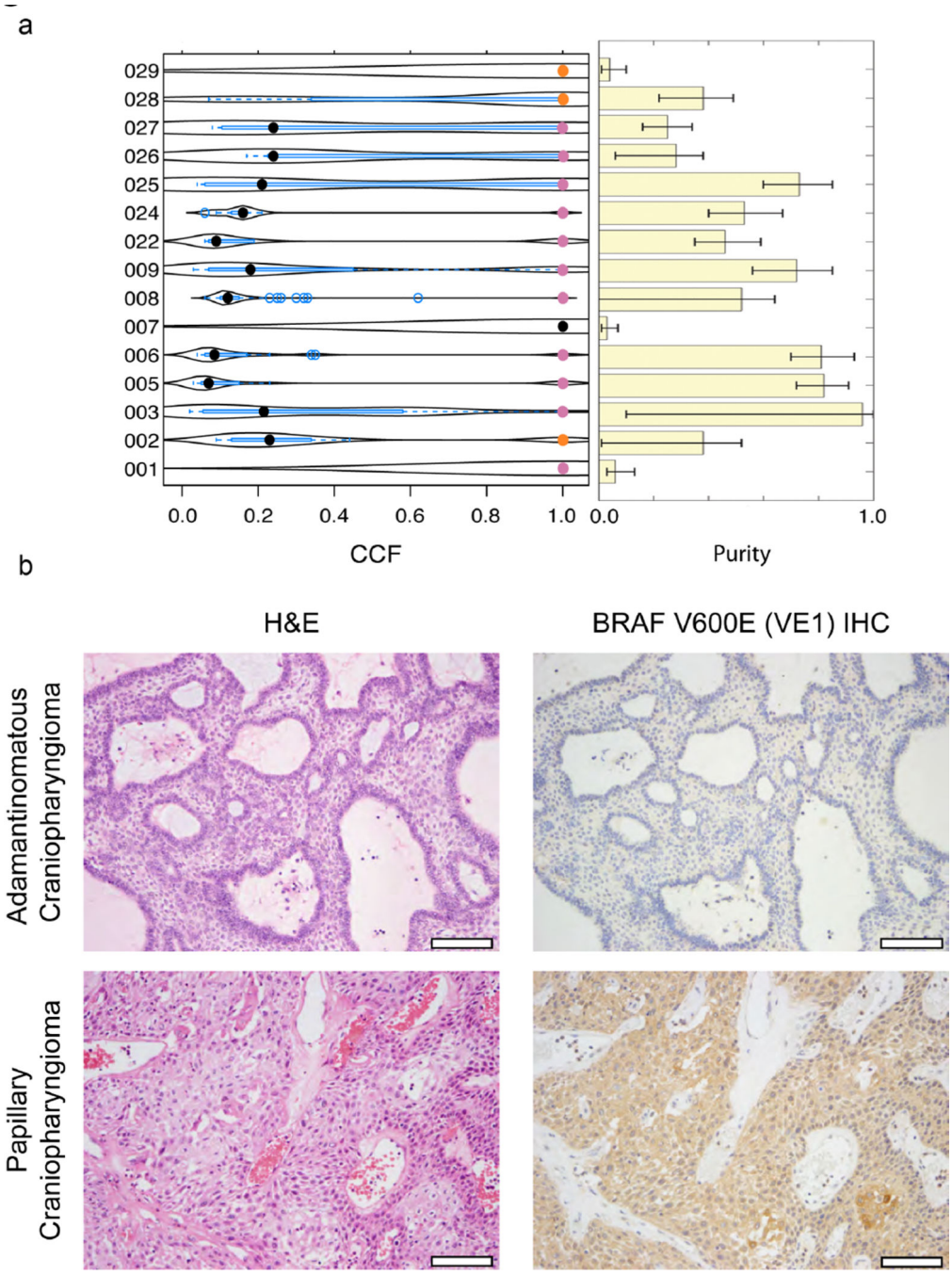

Figure 4.

BRAF and *CTNNB1* mutations are clonal in craniopharyngiomas. In Panel a (left), a violin plot shows the cancer cell fraction (CCF) for *BRAF* (orange) and *CTNNB1* (pink) mutations in each tumor analyzed with whole exome sequencing. The median CCF of all non-synonymous somatic mutations for each sample is represented by a black dot. The bar graph (Panel a, right) shows the computed purity for each sample (see Methods sections); error bars represent standard error of the mean. In Panel b, we show hematoxylin and eosin (H&E) staining of adamantinomatous and papillary craniopharyngiomas.

Immunohistochemistry (IHC) shows that adamantinomatous craniopharyngiomas are negative for BRAF V600E but that there is a diffuse distribution of BRAF V600E mutant protein in the neoplastic epithelium of papillary craniopharyngiomas. Stromal elements in the fibrovascular cores of the papillary tumors are negative for the BRAF V600E mutant protein. Scale bars, 100 μm.